Contents lists available at ScienceDirect

Desalination and Water Treatment

journal homepage: www.sciencedirect.com/journal/desalination-and-water-treatment/

Nanoparticles in wastewater: A comprehensive approach to understanding their ecotoxicity and genotoxicity

Nina Doskocz [a],[*] , Katarzyna Affek [a], Magdalena Matczuk [b], Marcin Drozd [c],[d] ,
Monika Załęska-Radziwiłł [a]

[a] *Department of Biology, Faculty of Building Services, Hydro and Environmental Engineering, Warsaw University of Technology, Nowowiejska 20, Warsaw 00-653, Poland*
[b] *Analytical Chemistry, Faculty of Chemistry, Warsaw University of Technology, Noakowskiego 3, Warsaw 00-664, Poland*
[c] *Centre for Advanced Materials and Technologies CEZAMAT, Warsaw University of Technology, Poleczki 19, Warsaw 02–822, Poland*
[d] *Medical Biotechnology, Faculty of Chemistry, Warsaw University of Technology, Noakowskiego 3, Warsaw 00–664, Poland*

A B S T R A C T

Herein, we investigated the impact of wastewater-borne Al_2O_3 nanoparticles (Al_2O_3NPs) on the aquatic organism *Daphnia magna*, focusing on both ecotoxicity and genotoxicity. The widespread use of nanoparticles (NPs) in various industries has raised concerns about their environmental effects, especially in wastewater. Our findings showed that exposure to Al_2O_3NP-containing wastewater, even after biological treatment, led to significant immobilization and reduced reproduction of *D. magna*. Additionally, changes in the genetic material of crustaceans were identified using RAPD-PCR (Random Amplified Polymorphic DNA) and TEM (Transmission Electron Microscopy), which revealed NP aggregates in the intestines, indicating the digestive tract as the primary site of NP uptake and possible cellular dysfunction. The hydrodynamic size of NPs increased post-treatment, and zeta potential measurements suggested a tendency for the nanomaterials to agglomerate. The concentration of dissolved aluminum ions also rose significantly after one day of biological wastewater treatment. These findings highlight the considerable risks wastewater-borne NPs pose to aquatic ecosystems and underscore the need for effective monitoring and risk management strategies to mitigate their environmental impact.

1. Introduction

The determination of the release pathway of nanoparticles (NPs) into the environment may be elaborated by their fate in wastewater treatment processes, which are released into municipal sewer systems. Upon reaching wastewater treatment plants (WWTPs), they may interact with microorganisms involved in biological treatment processes, thus affecting their efficiency. Moreover, in treated wastewater, NPs may occur in two phases: (1) suspended/dissolved in the aqueous phase and (2) adsorbed onto a solid matrix such as flocs of activated sludge, which indicates that they can enter the environment along with effluents from treatment plants (treated wastewater) or with used sewage sludge. Importantly, NPs are increasingly employed in wastewater treatment and water treatment processes, which increases their release into the environment [1–3]. According to Brar et al.[4] , NPs used in cosmetics were detected in wastewater in Sweden and Denmark at a rate of approx. 50 g per capita per day. In a city of one million people, the release of such NPs into wastewater was approx. 50 t per day [4]. Gottschalk et al. (2009) calculated the predicted environmental concentrations (PEC) based on a probabilistic material flow analysis from a life-cycle perspective of NP-containing products. PEC of Fullerenes, ZnONPs, AgNPs, and TiO_2NPs in WWTP effluents in the EU was 5.2, 0.4, 42.5, and 34.7 µg/L, respectively, which indicated that they were several magnitudes higher than the PEC for surface water, which was 0.017, 0.010, 0.764, and 0.015 µg/L, respectively [5].

However, despite the constant recommendations of scientists and representatives of international organizations regarding the urgent need for a comprehensive environmental risk assessment of NPs in wastewater, to date, only a few studies have been presented regarding the impact of NPs on aquatic and terrestrial ecosystem organisms after

passing through WWTP [6–9]. Most studies on the eco- and genotoxicity of NPs focus on pristine NPs such as Ag, AgO, and TiO_2, as well as ZnO, SiO_2, and CuO. These NPs disrupt enzyme functions, induce oxidative stress, and can cause developmental defects and increase mortality in aquatic organisms. They can also be toxic to aquatic plants, where they may interfere with plant growth and photosynthesis [1,5,10–12]. To the best of our knowledge, there are no studies on the toxicity of wastewater-borne NPs other than TiO_2 or AgNPs. Therefore, to meet EU requirements and develop a complete environmental risk profile related to the presence of nanomaterials (development of research methods, their standardization, and creation of ecotoxicological databases for used and newly manufactured nanomaterials), we focused on wastewater-borne Al_2O_3NPs. The purpose of this study was to investigate the effects of synthetic domestic wastewater-borne aluminum oxide nanoparticles (Al_2O_3NPs) before and after biological treatment in an SBR reactor on ecotoxicity in the crustacean *D. magna*. Since the majority of reports that examine the effects of wastewater-borne NPs are limited to ecotoxicity studies focusing on crustaceans and fish, usually considering survival or immobilization as endpoints, our research examines the molecular level. To evaluate the ecotoxicological effects, 48 h acute ecotoxicity and 21-day chronic ecotoxicity tests were conducted. RAPD-PCR analysis was carried out to understand the impact of the tested samples on the genetic material of crustaceans. RAPD-PCR (Random Amplified Polymorphic DNA - Polymerase Chain Reaction) is a molecular technique used to analyze genetic diversity and detect changes in genetic material. This method employs random primers to amplify DNA sequences, allowing the identification of polymorphisms within the genome. It is widely applied in genotoxicity studies, molecular ecology, and assessments of environmental stress impacts on living organisms [13]. Additionally, we conducted an ultrastructural study of *D. magna* cells after 48 h incubation with tested wastewater (using Transmission Electron Microscopy, TEM) to characterize possible internalization pathways or induced cellular dysfunctions. To assess the impact of Al_2O_3NPs in wastewater, the model lab-scale WWTPs (laboratory-scale sequencing batch reactors, SBRs) continuously fed with synthetic wastewater dosed with 10 mg/L Al_2O_3 NPs for 63 days were used. NPs found in wastewater may undergo many transformations during their treatment processes, hence, we utilized modern NP characterization techniques such as DLS (Dynamic Light Scattering) and spICP-MS/MS (Single Particle Inductively Coupled Plasma Mass Spectrometry/Mass Spectrometry). DLS is a technique used to determine the size distribution of small particles or molecules in suspension by measuring fluctuations in the intensity of scattered light caused by particle movement, and was used to determine the hydrodynamic diameters of NPs in suspensions (size of the nanomaterial metal-based core + any naturally occurring surface (bio)layers), their net charge (due to the measurement of the zeta potential), which allowed the estimation of the aggregation of nano-objects in the studied suspension, and the elaboration of the general dispersity of the studied population of NPs (polydispersity index, PDI) [14]. spICP-MS/MS is an advanced analytical technique used to detect, quantify, and characterize individual nanoparticles in a sample. It provides detailed information on particle size, concentration, and elemental composition by measuring the mass of individual particles. This method is widely applied in environmental monitoring, nanomaterial research, and contamination analysis. It was therefore used to characterise the most commonly present NP core size, with the size distribution of nanomaterials in solution, the number of particles per litre in samples and the amount of dissolved metal fraction [15].

The concentration of 10 mg/L for Al_2O_3 nanoparticles was selected based on concentrations reported in the literature for NPs detected in wastewater environments. Previous studies have shown that nanoparticle concentrations can vary widely depending on factors such as source, wastewater treatment efficiency, and environmental conditions. This concentration was chosen to simulate a worst-case scenario and ensure detectable ecotoxicological effects under laboratory conditions [16,17].

Our study contributes to a better understanding of the effects of wastewater-borne NPs on aquatic organisms and explains the relevant mechanisms of action of NPs and the critical data for assessing the potential ecological risks associated with using Al_2O_3 NPs. While this study focused on *D. magna* as a representative freshwater model, the observed toxicological mechanisms, such as bioaccumulation, oxidative stress, and DNA damage, are commonly reported across various taxa, including fish [18] and algae [19]. Therefore, our findings may provide valuable insights for assessing potential environmental risks in broader aquatic ecosystems.

2. Material and methods

2.1. Preparation of Al_2O_3NPs suspension

Commercial samples of Al_2O_3NPs (nanopowder < 50 nm with a specific surface area 40 m^2/g) and Al_2O_3 (bulk counterparts) with a purity over 98 % were obtained from Merck Life Sciences, Poznan, Poland (CAS no. 1344–28–1). Stock suspensions of 100 mg/L Al_2O_3NPs and Al_2O_3 were prepared as follows: 0.1 g NPs were placed in a 1 L volumetric flask, and the volume of NPs suspension was fixed to 1 L by adding Milli-Q water. Then, the NPs suspension was subjected to ultrasonic treatment (1 h) to break up the NPs agglomerates.

2.2. Lab-scale wastewater treatment plant (WWTP)

Wastewater from two model lab-scale WWTP (laboratory-scale sequencing batch reactors, SBRs) was used to perform the exposure experiments with *D. magna*. SBR bioreactors were seeded with sludge from a full-scale municipal WWTP ("Czajka", Warsaw, Poland) and operated for 63 d. After settling, the sludge was mixed with synthetic wastewater, and the initial mixed liquor-suspended sludge (MLSS) of the SBR was approx. 3500 mg/L. An influent pump was used to introduce synthetic wastewater into the SBR. The volume exchange ratio of the SBR was 50 % at each cycle. Briefly, the reactor cycle consisted of an anoxic/anaerobic period of 120 min (including 10 min of filling), an aerobic period of 190 min, a settling period of 40 min, and a decantation period of 10 min. This resulted in a total 6 h cycle and a hydraulic retention time (HRT) of 12 h. At the end of the aerobic period, the excess sludge was extracted daily as a mixed liquor to maintain MLSS of 3000–4000 mg/L.

During the anaerobic period, synthetic wastewater and activated sludge were mixed using

a magnetic stirrer, and in the aerobic period, air was introduced with spargers. According to Wang et al. (2017), the components of the synthetic wastewater with a slight adjustment were as follows (mg/L): CH_3COONa (510), $NaHCO_3$ (120), NH_4Cl (82), KH_2PO_4 (53), $ZnSO_4 \bullet 7H_2O$ (0.12), K_2HPO_4 (16), $MnCl_2 \bullet 4H_2O$ (0.12), $Na_2MoO_4 \bullet 2H_2O$ (0.06), $CuSO_4 \bullet 5H_2O$ (0.03), KI (0.03), H_3BO_3 (0.15), $CoCl_2 \bullet 6H_2O$ (0.15), and $FeCl_3 \bullet 6H_2O$ (1.5). The chemical oxygen demand (COD), soluble orthophosphate (SOP), and NH_4^+-N in the synthetic wastewater were approx. 400, 20, and 25 mg/L, respectively [20].

After an initial 2-week adaptation phase, synthetic wastewater with Al_2O_3NPs (10 mg/L) was added to one of the bioreactors. The second bioreactor – containing wastewater without nanoparticles – served as the control system (blank). Wastewater from all SBRs was collected weekly for the entire study period (63 days). The wastewater collected from the model WWTPs was shaken for 2 min before being used to obtain a homogeneous suspension. The list of wastewater samples used in the exposure experiments is provided in Table 1.

2.3. Characterization of Al_2O_3NPs in examined samples

DLS and ζ-potential measurements were performed on a Zetasizer

Table 1
Wastewater samples used in the exposure experiments with *D. magna.*

No	Samples collected for analysis	Sample name
1	Synthetic domestic wastewater-borne Al$_2$O$_3$NPs (10 mg/L), fed into the SBR reactor (Influent)	WW-NPs-I
2	Synthetic domestic wastewater (control), fed into the SBR reactor (Influent)	WW-Control-I
3	Synthetic domestic wastewater-borne 10 mg/L Al$_2$O$_3$NPs, treated by activated sludge method in SBR reactor after 1 day (Effluent)	WW-NPs-E/1d
4	Synthetic domestic wastewater-borne 10 mg/L Al$_2$O$_3$NPs, treated by activated sludge method in SBR reactor after 7 days (Effluent)	WW-NPs-E/7d
5	Synthetic domestic wastewater-borne 10 mg/L Al$_2$O$_3$NPs, treated by activated sludge method in SBR reactor after 14 days (Effluent)	WW-NPs-E/14d
6	Synthetic domestic wastewater-borne 10 mg/L Al$_2$O$_3$NPs, treated by activated sludge method in SBR reactor after 28 days (Effluent)	WW-NPs-E/28d
7	Synthetic domestic wastewater-borne 10 mg/L Al$_2$O$_3$NPs, treated by activated sludge method in SBR reactor after 42 days (Effluent)	WW-NPs-E/42d
8	Synthetic domestic wastewater-borne 10 mg/L Al$_2$O$_3$NPs, treated by activated sludge method in SBR reactor after 56 days (Effluent)	WW-NPs-E/56d
9	Synthetic domestic wastewater-borne 10 mg/L Al$_2$O$_3$NPs, treated by activated sludge method in SBR reactor after 63 days (Effluent)	WW-NPs-E/63d
10	Synthetic domestic wastewater without NPs (control), treated by activated sludge method in SBR reactor after 1 day (Effluent)	WW-Control-E/1d
11	Synthetic domestic wastewater without NPs (control), treated by activated sludge method in SBR reactor after 7 days (Effluent)	WW-Control-E/7d
12	Synthetic domestic wastewater without NPs (control), treated by activated sludge method in SBR reactor after 14 days (Effluent)	WW-Control-E/14d
13	Synthetic domestic wastewater without NPs (control), treated by activated sludge method in SBR reactor after 28 days (Effluent)	WW-Control-E/28d
14	Synthetic domestic wastewater without NPs (control), treated by activated sludge method in SBR reactor after 42 days (Effluent)	WW-Control-E/42d
15	Synthetic domestic wastewater without NPs (control), treated by activated sludge method in SBR reactor after 56 days (Effluent)	WW-Control-E/56d
16	Synthetic domestic wastewater without NPs (control), treated by activated sludge method in SBR reactor after 63 days (Effluent)	WW-Control-E/63d

Nano ZS device (Malvern Panalytical, UK) to determine the average hydrodynamic diameter (dH), size distribution, surface charge, and polydispersity index (PDI). The wastewater suspensions were diluted 200 times with ultrapure water before measurement to obtain optimal scattering intensity. The measurements were carried out in disposable polystyrene cuvettes previously thermostated for 120 s to reach a temperature of 25 °C. A dip cell equipped with palladium electrodes was employed for the ζ-potential studies. All size and ζ-potential measurements were carried out in four replicates.

spICP-MS/MS measurements were performed on an Agilent 8900 ICP Triple Quadrupole Mass Spectrometer (Santa Clara, USA) equipped with Single Nanoparticle Application Module software. The instrument was equipped with Pt sampling and skimmer cones, a MicroFlow nebulizer, a Scott spray chamber, and a quartz torch with a 1.5 mm i.d. injector. Samples were introduced directly into the ICP-MS/MS with the standard peristaltic pump. A series of dilutions were performed on the samples with deionized water to produce particle concentrations of 50,000–300,000 particles/mL (as measured during analysis), diluted 20-fold. Analyses were performed in the Time-Resolved Analysis (fast TRA) mode, using a dwell time of 0.1 ms (100 μs) per point with no settling time between measurements. The RF power was 1550 W, nebulizer gas flow – 0.95 L min^{-1}, collision/reaction gas flow (hydrogen) – 5.0 mL min^{-1}, sample depth 8.0 mm, and monitored isotopes: ^{27}Al (on-

mass mode). The working conditions were optimized daily using a 10 μg L^{-1} solution of ^{59}Co$^+$, ^{89}Y$^+$, and ^{205}Tl$^+$ in 2 % (v/v) HNO$_3$. The gold nanoparticle standard reference material with a nominal diameter of 50 nm (EM.GC50/4, Gold Colloid) was used to determine transport efficiency, which was calculated using the particle frequency method [21]. The sample flow rate was calculated daily by measuring the mass of water taken up by the peristaltic pump for 2 min (this operation was repeated 3 times). The Agilent dedicated software automatically processed raw data, but we additionally verified the correctness of the established threshold parameter. The software generated the median particle size, number of particles per L, size distribution, and information about the dissolved metal concentration. All measurements were carried out in three replicates. The obtained final values were calculated, considering the results registered for analogical control samples.

2.4. Exposure of D. magna to the wastewater from model WWTPs

2.4.1. Test species and culture conditions

The freshwater crustacean *D. magna* Strauss was used as a model species. The crustaceans were obtained from the laboratory culture of the Department of Biology, Faculty of Building Services, Hydro, and Environmental Engineering, Warsaw University of Technology. Organisms were kept in permanent in-house breeding at 20 ± 2 °C with a 16:8 h light-dark cycle, using 15 L glass aquariums filled with artificial freshwater under the conditions described in the guidelines of the OECD 211 [22]. The culture medium was renewed weekly. Cultured daphnia animals were fed daily with *Chlorella vulgaris* algae (1.5–2.5 × 10^8 cells/d). The above conditions assure continuous parthenogenetic reproduction in cultures.

2.4.2. Acute and chronic ecotoxicity tests

Two assays were used to evaluate the tested wastewater's short-term and chronic toxicity effects on *D. magna*. Immobilization tests (acute tests) with juvenile forms of the crustacean Daphtoxkit F™ were carried out according to the methodology described in the instructions of Microbiotests (Belgium) (with modifications). Procedures adhered to OECD 202 guidelines [23]. Determination of the number of immobilized organisms was conducted after 24 and 48 h of contact with the tested wastewater samples. After 48 h of incubation with treated wastewater samples, live bioindicators were collected for DNA extraction. The crustacean reproduction tests (chronic tests) were carried out according to OECD 211 (2012) methodology under semistatic conditions with daily replacement of solutions [22]. Test was performed in 24-well polystyrene plates with 10 mL of test solution and for the control. Exposure of organisms to the polystyrene microbeads lasted 21 d. The offspring was counted daily and removed from the test vessels. The experiment was run under laboratory conditions at 20 ± 2 °C, and 16 h light:8 h dark.

The experiments was performed in triplicate to ensure reproducibility and reliability of the results. Mean values for the number of immobilized organisms and the number of neonates were compared using a pairwise Student's *t*-test to evaluate the significance of differences between the control and treatment groups (p < 0.05).

2.4.3. RAPD procedures

DNA was extracted from live *D. magna* individuals collected after the 48-hour immobilization test. The RAPD-PCR test was performed to evaluate the effects of the tested wastewater at a molecular level. The procedure previously described in our research group was used to process the daphnids [24–26]. All RAPD-PCR chemicals were purchased from A&A Biotechnology (Gdańsk, Poland). Total DNA from *D. magna* was extracted and purified using DNA-XpureTM Cell micro using the manufacturer-supplied protocol. The DNA profiles of crustaceans were generated in RAPD-PCR reactions performed in a reaction volume of 25 μL. The decamer oligonucleotides (primers) OPB7 (GGTGACGCAG), OPB8 (GTCCACACGG), OPA9 (GGGTAACGCC), and OPB10

(CTGCTGGGAC) were obtained from Environmental Laboratory of DNA Sequencing and Synthesis IBB PAS (Warsaw, Poland). One of the primers was used for each amplification. Approx. 25 ng of *D. magna* genomic DNA was subjected to RAPD amplification with reaction mixtures containing PCR Mix (0.1 U/μL Taq DNA polymerase, 4 mM, MgCl$_2$, 1xPCR Buffer, 0.5 mM of each dNTP) (A&A Biotechnology, Poland) and a primer concentration of 10 μM. Amplifications were performed in DNA thermocycler (Mastercycler pro, Eppendorf) programmed for 4 min at 95 °C (initial denaturation), 39 consecutive cycles each consisting of 1 min at 95 °C (denaturation), 1 min at 40 °C (annealing), 1 min at 74 °C (extension), and followed by 1 cycle for 10 min at 74 °C (final extension). Control PCRs lacking genomic DNA were conducted for every set of samples. Reaction mixtures were kept at 4 °C before use.

After amplification, RAPD reaction products were analyzed by electrophoresis on 1 % agarose gels in 1 × Tris-Borate-EDTA buffer (40 mM Tris base, 20 mM boric, and 1 mM EDTA) at 80—100 V for approx. 30–50 min in SUBDNA apparatus (Kucharczyk, Poland). GeneRuler 1 kb DNA Ladder (Fermentas, USA) was used as a molecular weight DNA standard. DNA bands were stained with ethidium bromide, visualized, and photographed under UV light. Digital processing of the images and computational analysis were performed using GelDoc-It Imaging System (UltraViolet Products Ltd, USA). All amplifications were repeated twice to confirm their reproducibility of RAPD patterns. Only repeatable and clear amplification bands were scored for constructing the data matrix.

The effect of wastewater-borne NPs (as well as the control) on the genetic material of *D. magna* before and after the biological treatment process was assessed by the genetic similarity index of bands' profiles (S, %) and genetic stability of DNA (GTS, %) between tested and control samples for individual primers. The genetic similarity index (S, %) was calculated as the proportion of amplification products that were not polymorphic concerning the total number of amplified products, *2 × number of shared fragments/total number of fragments* [27,28]. Genomic template stability (GTS, %) was calculated for each primer as the formula: *100 – (100a/n)* where a was the average number of changes in DNA profiles of each sample tested and *n* the total number of bands in the control DNA profiles. Polymorphism observed in RAPD profiles included the disappearance of a normal band and the appearance of a new band compared to control (negative and positive) RAPD profiles [29,30]. Mean values and standard deviations were calculated. Changes in these values were calculated as a percentage of the negative control (set to 100 %) and allowed to distinguish organisms exposed to genotoxic agents.

2.4.4. Ultrastructural analysis of D. magna

To investigate the interaction of Al$_2$O$_3$NPs from wastewater and *D. magna* cells, Transmission Electron Microscopy (TEM) images of crustaceans exposed to the tested samples were acquired. The alive cells of *D. magna* from tested wastewater samples were collected before incubation and after 48 h and kept at 4 °C. Cells of daphnids were fixed with 2.5 % glutaraldehyde cacodylic buffer and incubated for 1 h, then washed in 0.1 M cacodylic buffer. Next, the cell was postfixed in 1 % OsO$_4$ in ddH$_2$O for 1 h and washed three times in ddH$_2$O. After postfixation, the samples were dehydrated through a graded series of EtOH (30 % - 10 min, 50 % - 10 min, 70 % - 24 h, 80 % - 10 min, 90 % - 10 min, 96 % - 10 min, anhydrous EtOH - 10 min, acetone - 10 min), infiltrated with Epon resin in acetone (1:3–30 min, 1:1–30 min, 3:1–2 h), infused twice for 24 h in pure Epon resin, and polymerized 24 h at 60 ℃. Next, 60 nm sections were prepared (RMC ultramicrotome MTX) and contrasted with uranyl acetate and lead citrate according to Reynollds (1983) and were examined on a LIBRA 120 electron microscope produced by Zeiss [31]. Images were captured by the Slow Scan CCD (Proscane) using EsiVision Pro 3.2 software (Soft Imaging Systems GmbH). Measurements were performed using the analySIS® 3.0 image-analytical software (Soft Imaging Systems GmbH). For the TEM analysis, 25 images were examined for each experimental sample,

focusing on particle morphology and aggregation behavior.

3. Results and discussion

3.1. NPs size

The hydrodynamic size of Al$_2$O$_3$NPs in wastewater after treatment ranged from 43.1 ± 6.67–615.1 ± 45.30, as determined by DLS (Fig. 1). The size of the Al$_2$O$_3$ core of the nanoobjects ranged from 32 ± 0.17–50 ± 0.18 nm as determined by spICP-MS/MS (Table 3). Interestingly, for samples collected during 1—14 days of treatment, the obtained values measured by both techniques indicated the comparable stability of hydrodynamic and core size values. After that time, we observed an increase in median core size (accompanied by a decrease in the dissolved metal concentration and NP number growth) and elevated nanomaterial hydrodynamic size. The first phenomenon possibly stemmed from the secondary build-up of particles when the dissolved Al concentration was high in the suspension. At the same time, the enhanced hydrodynamic diameter was due to the interactions of matrix wastewater components with the surface of building-up particles.

3.2. Zeta (ζ) potential of nanoparticles

ζ-potential refers to the electric potential at the boundary between the stationary layer of fluid attached to a charged particle and the surrounding bulk fluid. It is a crucial indicator of colloidal stability. A high absolute value of zeta potential (either positive or negative) signifies strong electrostatic repulsion between particles, reducing the likelihood of aggregation. Conversely, a low zeta potential indicates weaker repulsive forces, increasing the risk of particle agglomeration [32]. From the zeta-potential values of the analyzed nanoparticles in wastewater before treatment, we can observe that Al$_2$O$_3$NPs generally possess relatively higher stability (lower absolute value of zeta potential) than the Al$_2$O$_3$NPs in wastewater after treatment. However, it has been observed that the zeta potential value of Al$_2$O$_3$NPs in wastewater after treatment ranged from about −11.29 mV to −22.66 mV. In the initial stages of wastewater treatment (till 7 days), the obtained values indicate the lower agglomeration possibility, while during the second part of the experiment, the lower absolute values of zeta potential can be taken in the opposite manner (Fig. 2). Once more, the observed changes can be explained by the higher involvement of other sample (bio)compounds in interactions with nanoparticle surface (changes in net charge of nanoobjects).
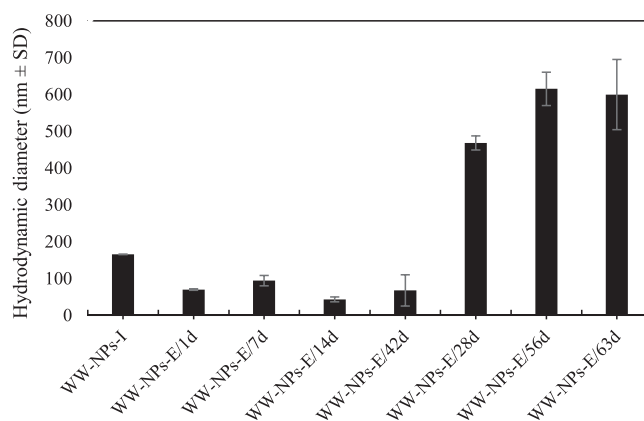

Fig. 1. Characterization of Al$_2$O$_3$NPs average hydrodynamic size in synthetic wastewater and effluents collected during 63 days of dosing of the system determined using DLS analyses. Error bars illustrate standard errors.
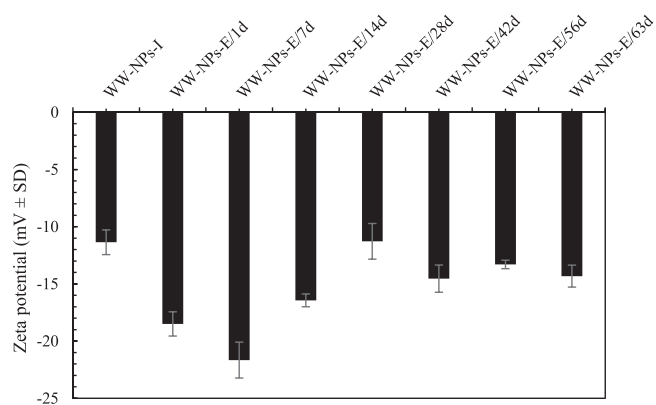
Fig. 2. Zeta potential of Al$_2$O$_3$NPs in synthetic wastewater and effluents collected during 63 days of dosing of the system determined using DLS analyses. Error bars illustrate standard errors.

3.3. Polydispersity index (PDI)

PDI is a critical indicator of the monodispersity of the nanoparticle population in the measured sample. Low PDI values (< 0.1) indicate a narrow size distribution, meaning the particles are highly uniform in size, in turn high PDI values (> 0.3) prove the broad size distribution and low prediction of suspension behavior [33,34]. PDI values for Al$_2$O$_3$NPs in wastewater before treatment were calculated as 0.22 – the nanomaterial was rather monodispersed. For Al$_2$O$_3$NPs in wastewater after treatment, they were in the range of 0.44–0.75 and increased with the duration of the test, which once more confirms the idea of nanoparticles re-construction after a more extended time of biological wastewater treatment (Fig. 3).

3.4. The concentration of diluted Al fraction

The obtained number of particles per liter for wastewater-borne Al$_2$O$_3$NPs before treatment was 5.19×10^9, while the concentration of dissolved Al was very low – 0.6 ng/mL. In the first part of the experiment, the rapid decomposition of NPs was noted (to 1.12×10^9), accompanied by high dissolved Al concentrations in suspensions. Then, the NPs were re-built (a decrease in Al value and an increase in core size and number of particles). After 28 days of wastewater treatment, the number of particles decreased (while Al concentration increased), supporting that high matrix components impact the nanochemistry of the suspension (Table 2).
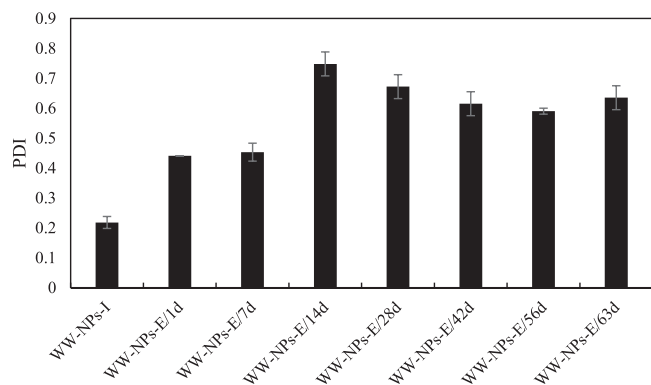

Fig. 3. PDI of Al$_2$O$_3$NPs in synthetic wastewater and effluents collected during 63 days of dosing of the system determined using DLS analyses. Error bars illustrate standard errors.

Table 2
Median size of NPs, NPs number concentration, and concentration of dissolved Al in synthetic wastewater and effluents collected during 63 days of dosing of the system determined using spICP-MS/MS analyses.

	Diameter/nm	NPs number concentration/L	Al (ng/mL)
WW-NPs-I	38	5.19×10^9	0.600
WW-NPs-E/1d	32	1.12×10^9	77.78
WW-NPs-E/7d	34	1.14×10^9	54.34
WW-NPs-E/14d	38	1.74×10^9	50.62
WW-NPs-E/28d	52	5.55×10^9	7.400
WW-NPs-E/42d	50	2.78×10^9	19.00
WW-NPs-E/56d	42	1.86×10^9	28.02
WW-NPs-E/63d	36	1.12×10^9	34.84

3.5. Effects of wastewater on the immobilization and reproduction of D. magna

The influence of all tested wastewater samples on the immobilization of *D. magna* crustaceans was observed. Wastewater with Al$_2$O$_3$NPs fed into the bioreactor (WW-NPs-I) influenced the immobilization of crustaceans to a lesser extent. The percentage of immobilization ranged from 19 % to 22 % for all samples tested. A similar effect was observed in the control wastewater (WW-Control-I) (Fig. 4). Significant immobilization of *D. magna* was found after exposure to wastewater-borne Al$_2$O$_3$NPs (WW-NPs-E), collected at 56 and 63 days after wastewater treatment (36 % and 34 % greater immobilization, respectively, compared to WW-Control-E). In turn, the control wastewater treatment had significantly less impact on the immobilization of *D. magna* (Fig. 4). The difference in the inhibition of immobilization of the bioidentifiers between WW-Control-I and WW-Control-E was 1 %–10 %. It was shown that despite treating wastewater containing Al$_2$O$_3$NPs, it still affects the immobilization of the tested bioindicators.

We found that all tested wastewater samples affected the reproduction of *D. magna* crustaceans. Wastewater with Al$_2$O$_3$NPs fed into the bioreactor (WW-NPs-I) had less influence on the reproduction of crustaceans than WW-NPs-E. The number of cumulative offspring per surviving adult was 19. A similar effect was observed in the control wastewater (WW-Control-I) (Fig. 5). The number of cumulative offspring per surviving adult was reduced by 10.5 %, 16.1 %, 14.0 %, 28.1 %, 28.7 %, and 30.6 % in the presence of treated wastewater collected after 7, 14, 28, 42, 56, and 63 days compared to WW-Control-I, respectively (Fig. 5). In turn, the treatment of the control wastewater increased the number of cumulative offspring per surviving adult individual (Fig. 5). Despite treating wastewater containing Al$_2$O$_3$NPs, the reproduction of the tested bioindicators was affected.

3.6. Effects of wastewater on the genetic material of D. magna

The RAPD-PCR reaction of the genetic material of *D. magna* crustaceans exposed to tested wastewater samples for 48 h resulted in amplification products with characteristic patterns visualized as bands after electrophoresis (so-called fingerprints). An example of the DNA band profiles obtained for OPA7 primer is shown in Fig. 6. Changes occurred in the patterns of the reaction products in all samples compared to the negative (water) and positive control (0.01 % DMF).

Several qualitative changes in the DNA band profile (RAPD pattern) were observed using different primers for all tested wastewater compared to the control. Observed polymorphisms included the appearance of new bands and the disappearance of expected bands, indicating genetic modifications in the tested samples compared to controls. These changes suggest genotoxic effects caused by exposure to nanoparticles present in the wastewater samples [24,29].

The degree of genetic similarity (S) of the amplification products (concerning the negative and positive control) obtained for the wastewater before treatment differed from the profile of the bands obtained for the sewage after treatment. Despite treating wastewater containing
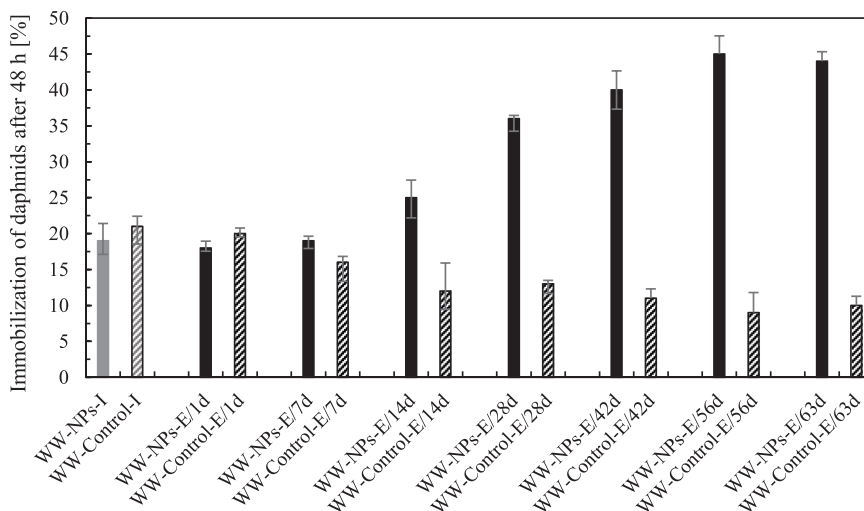
Fig. 4. Immobilization percent (%) after 48 h of the *D. magna* after exposure to tested wastewater. Error bars illustrate standard errors.
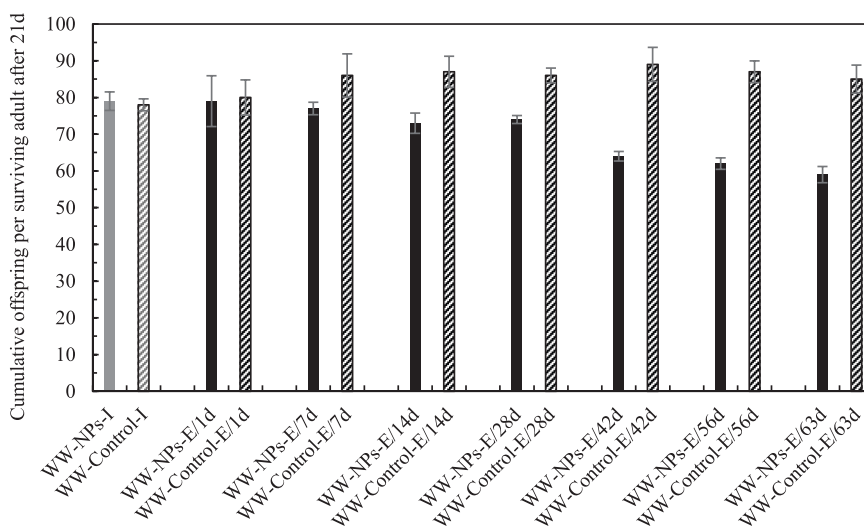

Fig. 5. Reproduction of *D. magna* after 21 days of exposure to tested wastewater. Error bars illustrate standard errors.

Al$_2$O$_3$NPs, changes in the genetic material of bioindicators occurred. The S value for treated wastewater relative to raw wastewater (before treatment) with Al$_2$O$_3$NPs ranged from 57 % to 86 % for all primers. Initially, this value increased until 42 day of biological wastewater treatment, where a decrease began (Table 3). The lowest degree of genetic similarity was found in the presence of WW-NPs-E/63d and differed from the negative and positive control by 22 % and 44 %, respectively. Based on the GTS value, wastewater containing Al$_2$O$_3$NPs after biological treatment had a greater impact on the genetic material of *D. magna*. The average GTS value ranged from 42.5 % to 80 %. The lowest GTS value was obtained in the presence of WW-NPs-E/63d and differed from the negative and positive controls by 57.5 % and 2.5 %, respectively (Table 3).

The control wastewater had less impact on the DNA of bioindicators. The S value was 56 % in the presence of WW-Control-I and ranged from 57 % to 100 % for treated wastewater (WW-Control-E). The S and GTS values in the presence of the control wastewater (WW-Control-E) were similar to those obtained in the presence of the negative control. The S value showed a significant difference only at the beginning of the treatment process compared to the negative control and amounted to 56 %, while the GTS value was 65 % (negative control 100 %). The degree of generic similarity in *D. magna* in the presence of treated

wastewater after 28 d, 42 d, 56 d, and 63 d was comparable to the control. In contrast, GTS differed by 21.2 %, 8.7 %, 8.7 %, and 3.7 %, respectively.

3.7. Microscopy TEM

Fig. 7 shows the TEM images of the cross-sectioned guts of *D. magna* exposed to water (control, to show the typical cell structure of the crustaceans), wastewater with Al$_2$O$_3$NPs before treatment, and wastewater without NPs before treatment.

BM = basement membrane; V = vacuole; black arrowhead = lateral plasma membrane; black arrow = nanoparticles.

In turn, Fig. 8 presents TEM images of *D. magna* exposed to WW-NPs-E. After exposure to the tested samples, nanoparticles were found in crustacean cells. This analysis evidenced NPs in the intestinal epithelium, suggesting the digestive tract as a crucial target and uptake site for NPs in *D. magna*. A higher number of NPs were observed in crustacean cells following their exposure to treated wastewater compared to exposure to sewage before treatment (Fig. 8). Nanoparticles were observed: (1) among and inside microvilli; (2) inside the cytoplasm; (3) into mitochondria as well as in some endosomes; (4) in the paracellular space. ESI analyses confirmed the aluminium composition of these NPs.
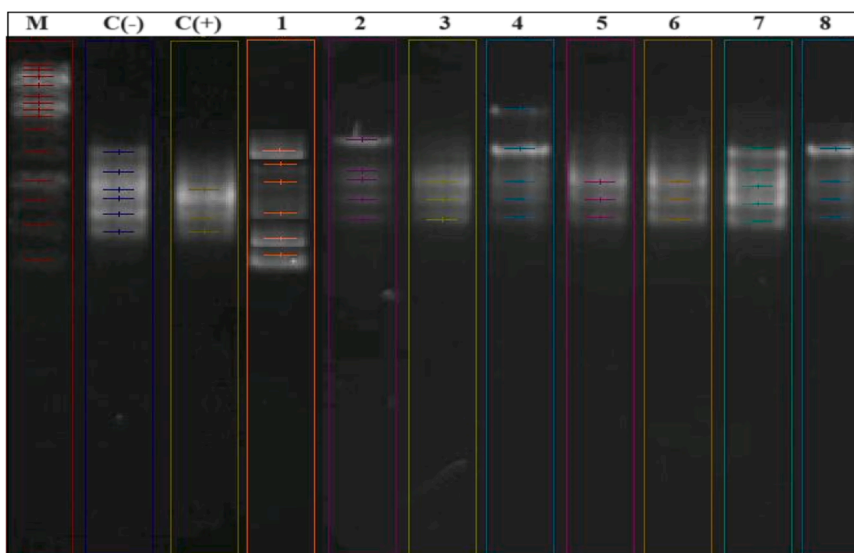
Fig. 6. Example diagram of the genetic similarity of RAPD-PCR reaction products using genetic material of *D. magna* crustaceans incubated in the presence of water (negative control – C(-)), 0.01 % DMF (positive control – C(+)), WW-NPs-I (1), WW-NPs-E/1d (2), WW-NPs-E/7d (3), WW-NPs-E/14d (4), WW-NPs-E/28d (5), WW-NPs-E/42d (6), WW-NPs-E/56d (7), WW-NPs-E/63d (8) using OPB7 primer. M = DNA size marker GeneRuler 1 kb DNA Ladder (VisionWorksLSM program).

Table 3

The values of the degree of similarity of obtained profiles (S, %) and Genetic stability (GTS, %) of *D. magna* RAPD bands exposed to tested wastewater concerning negative control (water) and positive control.

Sample	Mean* S value [%]	Mean* GST value [%]
WW-NPs-I	57	68.8
WW-Control-I	56	65.0
WW-NPs-E/1d	57	65.0
WW-Control-E/1d	56	66.3
WW-NPs-E/7d	57	78.8
WW-Control-E/7d	80	82.5
WW-NPs-E/14d	78	80.0
WW-Control-E/14d	80	77.5
WW-NPs-E/28d	86	76.3
WW-Control-E/28d	100	78.8
WW-NPs-E/42d	86	66.5
WW-Control-E/42d	100	91.3
WW-NPs-E/56d	80	56.3
WW-Control-E/56d	100	91.3
WW-NPs-E/63d	78	42.5
WW-Control-E/63d	100	96.3
C(-)	100	100
C(+)	34	45

* Average calculated from all tested primers

Fig. 9 presents the TEM images of *D. magna* exposed to wastewater from the control SBR after treatment. After incubation with influents, TEM images of *D. magna* showed only organic contaminants visible as dark spots/structures (Fig. 9).

Our results indicated that despite the biological process of wastewater treatment, Al_2O_3NPs remained in the treated wastewater and, after reaching the recipient, may affect aquatic organisms such as *D. magna* (Figs. 4–6, Table 3). Contrary to our expectations, wastewater-borne NPs showed a greater ability to immobilize, inhibit reproduction, and cause DNA damage in *D. magna* crustaceans compared to those in wastewater before treatment. Few studies have also demonstrated that nanoparticles can significantly affect the survival and reproduction of *D. magna*. Kowalska-Góralska and Nowak (2023) reported that copper nanoparticles adversely impact *D. magna*, with smaller particle sizes and higher concentrations causing increased mortality [35]. Similarly, ZnONPs have been shown to reduce both survival and reproductive capacity, indicating strong toxicological effects [36,37]. Additionally, AgNPs, known for their antibacterial properties, can disrupt aquatic ecosystems. Studies by Silva et al. (2021) revealed that AgNPs reduce survival and reproductive success in *D. magna*, leading to ecological imbalances in freshwater environments [38]. Also, Zhu et al. (2001) corroborated our findings, where they examined the effect of TiO_2NPs on *D. magna* and showed minimal toxic effects after 48 h, significant toxicity in *D. magna* exposed to TiO_2NPs after 21 days and accumulation of NPs inside crustacean cells. They attributed this chronic toxicity to the
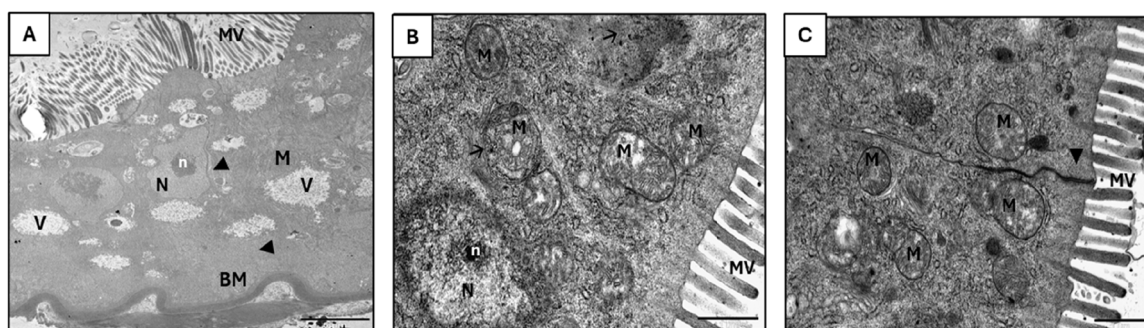

Fig. 7. TEM images from the midgut of controls (A), WW-NPs-I (B), and WW-Control-I (C) exposed samples. MV = microvilli; M = mitochondrion; MLB = multilamellar body; N = nucleus; n = nucleolus;.
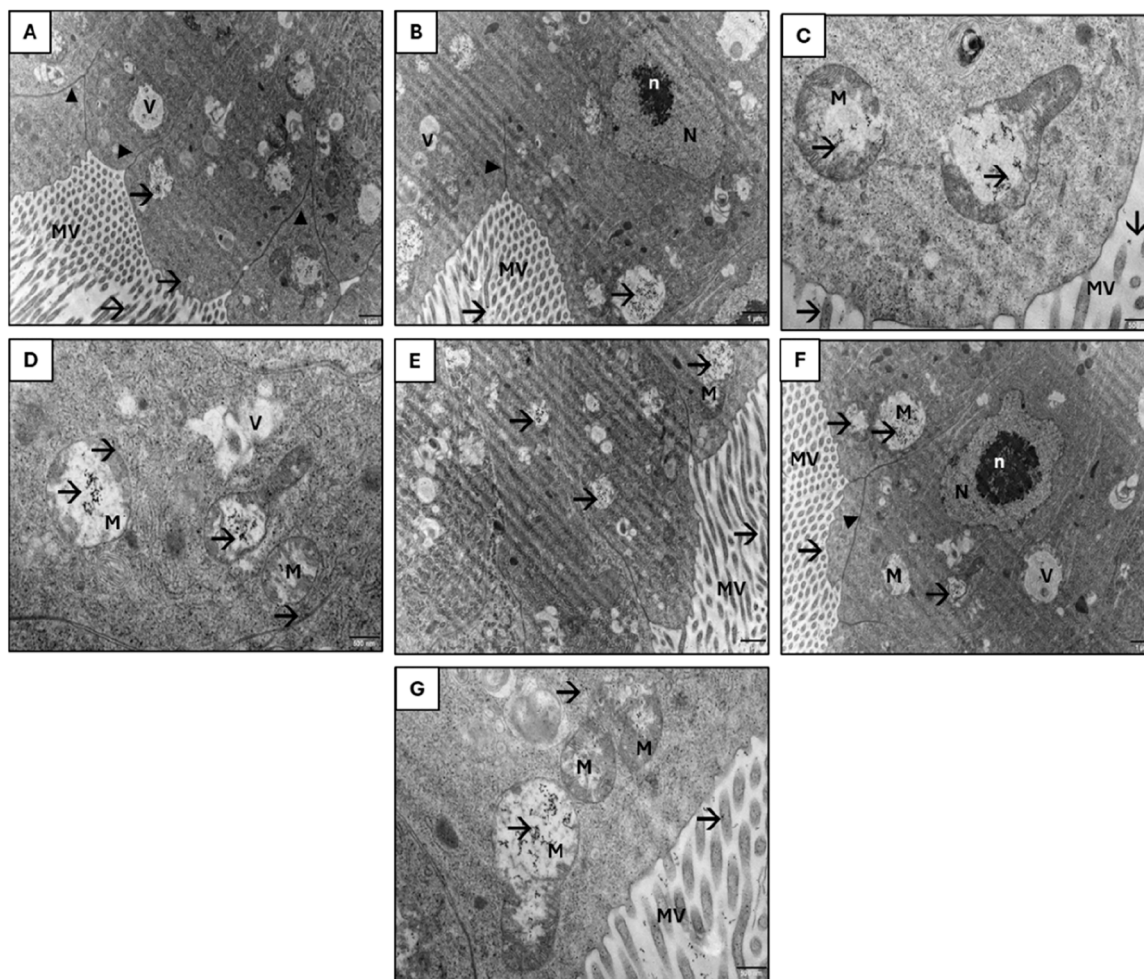
Fig. 8. TEM images from the midgut of WW-NPs-E after 1d (A), WW-NPs-E/7d (B), WW-NPs-E/14d (C), WW-NPs-E/28d (D), WW-NPs-E/42d (E), WW-NPs-E/56d (F) and WW-NPs-E/63d (G) exposed samples. MV = microvilli; M = mitochondrion; N = nucleus; n = nucleolus; V = vacuole; black arrowhead = lateral plasma membrane; black arrow = nanoparticles.

interference of bioaccumulated NPs with food intake [39]. Recent research has demonstrated that nanoparticles can disrupt survival and reproduction in fish and other aquatic organisms. For instance, studies of Kakakhel et al. (2021) on the effects of AgNPs on *Cyprinus carpio* have shown that prolonged exposure to high concentrations of these nanoparticles leads to liver damage and immune system dysfunction in fish [40]. In turn, Malhotra et al. (2020) analyzed the available toxicological profiles of copper ions and CuNPs in various fish species. The authors concluded that the toxicity of CuNPs depends on physicochemical factors such as water hardness, alkalinity, the presence of inorganic and organic ligands, pH, and temperature. Exposure of rainbow trout (*Oncorhynchus mykiss*) to CuNPs was shown to result in increased fish mortality associated with gill and liver damage and osmotic imbalance. Similar effects were observed in zebrafish (*Danio rerio*), where CuNPs caused oxidative stress and DNA damage, leading to reduced survival. [41]. The neurotoxic effects of CuNPs on *D. rerio* embryos were also investigated. The results showed that CuNPs exposure induced oxidative stress, inflammatory response, and impaired neurodevelopment in embryos [42].

A reason for the ecotoxic effects may be genetic changes caused by NPs. It should be noted that RAPD-PCR analysis revealed significant genetic changes in crustaceans in the presence of the tested samples, which indicates potential genotoxic effects of nanoparticles. The appearance of new DNA bands suggests the activation of previously inactive genomic regions, while the disappearance of existing bands may indicate deletions or damage to primer-binding sites, leading to

genomic structure disruptions [29]. Band intensity changes may result from altered copy numbers of certain sequences, reflecting disruptions in DNA replication and repair processes. These observations align with previous studies showing that metal nanoparticles can induce DNA damage, leading to point mutations, deletions, and other genetic aberrations [24–26,29]. Ellis et al. (2020) showed that AgNPs caused significant reductions in S% and GTS% in *D. magna*, indicating DNA damage through increased polymorphism and decreased genomic stability [43]. Similarly, ZnONPs triggered reductions in GTS% and changes in RAPD profiles in *Lemna minor*, showing direct genotoxic effects [12]. Our previous studies also showed that Al_2O_3NPs disrupted genetic stability in *Pseudomonas putida*, decreasing S% and GTS% due to DNA alterations induced by nanoparticles [26].

It is believed that the ecotoxic and genotoxic effects may result from the deposition of nanoparticles in crustacean cells, as confirmed by TEM analysis, which demonstrated the ability of Al_2O_3NPs to penetrate the gut cells of *D. magna*, with the main localization sites being the microvilli and mitochondria. The accumulation of nanoparticles in these organelles can interfere with essential cellular functions such as energy production and ion regulation, potentially leading to increased oxidative stress and cellular damage. The presence of nanoparticles in mitochondria may disrupt their metabolic function, leading to organelle swelling and cristae disintegration. Such changes can impair cellular respiration processes, ultimately causing apoptosis [44,45]. These findings are consistent with previous studies on the toxicity of metal nanoparticles in aquatic ecosystems. Bruneau et al. (2016) demonstrated that AgNPs
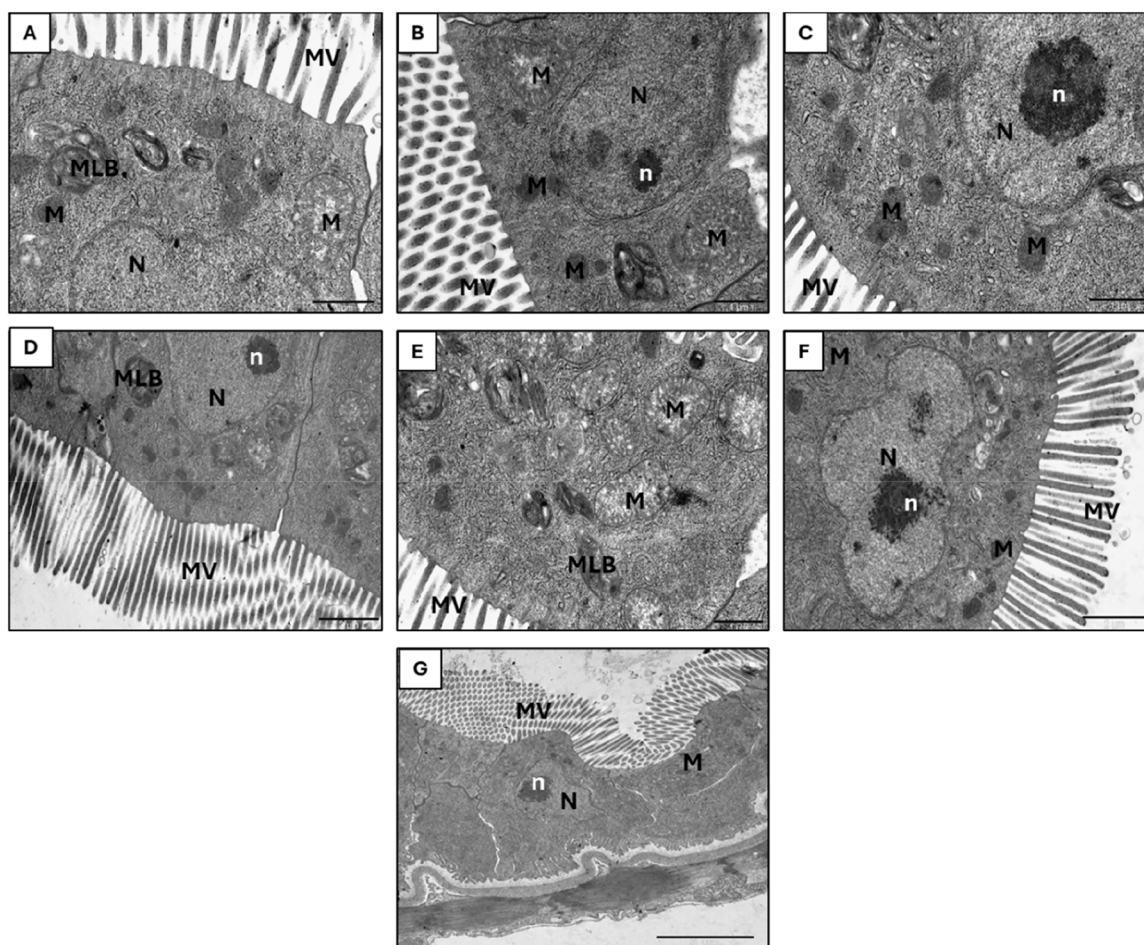
Fig. 9. TEM images from the midgut of WW-Control-E/1d (A), WW-Control-E/7d (B), WW-Control-E/14d (C), WW-Control-E/28d (D), WW-Control-E/42d (E), WW-Control-E/56d (F) and WW-Control-E/63d (G) exposed samples. MV = microvilli; M = mitochondrion; N = nucleus; n = nucleolus; V = vacuole; MLB = multilamellar body; black arrowhead = lateral plasma membrane.

accumulate in fish cells, causing mitochondrial damage [18]. Santo et al. (2014) also showed the presence of ZnONPs in the tissues of *D. magna* (in microvilli, endocytic vesicles near the upper surface of cells, mitochondria, free in the cytoplasm and the paracellular space between adjacent cells) although after 48 h acute toxicity tests were conducted for two types of ZnONPs (<100 nm and <50 nm) and showed minor effects, with EC_{50} values of 3.1 mg/L (<100 nm) and 1.9 mg/l (<50 nm) [46]. Similar results were obtained by Kwon et al. (2014), where Fe_3O_4NPs and α-Fe_2O_3NPs caused a crucial disturbance in microvilli and bacterial colonization of the gut lumen, although significant acute toxicity to *D. magna* was not observed [47]. Kwon et al. (2014) and Santo et al. (2014) suggested that the NPs causing these effects may disrupt ion transport processes and impair the synthesis of digestive enzymes, thereby disturbing metabolism and chemical transformations in the digestive tract [46,47]. Lovern et al.[48] explained that the inhibition of growth, survival (immobilization), or possibly the reproduction of *D. magna* crustaceans may stem from the presence of NPs in the intestines. This inhibits the absorption of nutrients because of the obstruction caused, or from the consumption of a large amount of energy to remove NPs from the intestines [48]. Kakakhel et al. (2021) showed that AgNPs caused histopathological changes in *C. carpio*, including tissue necrosis and mitochondrial damage due to bioaccumulation in the liver, gills, and intestines [40]. In turn, graphene oxide NPs disrupted cell walls and caused DNA fragmentation in freshwater algae [49], while TiO_2NPs damaged chloroplast membranes in *Chlorella vulgaris*, impairing photosynthesis [50].

Furthermore, it should be noted that a higher amount of NPs from

wastewater was observed in *D. magna* cells after incubation with treated wastewater than after incubation with wastewater flowing into the SBR. Our results showed that NPs were present in large quantities in the wastewater flowing into the bioreactor (Table 2) and that their interaction with the matrix components, both chemical and biological, was possible. In addition, NPs could be retained by the filtration mechanisms of *D. magna* and do not penetrate (or penetrate but at lower levels) into the cells [39].

Our results indicate that changes in the hydrodynamic size and ζ-potential of Al_2O_3 nanoparticles (Al_2O_3NPs) after wastewater treatment significantly affect their mobility, stability, and interactions with aquatic organisms such as *D. magna*. Hydrodynamic size determines the nanoparticles' ability to remain suspended in water. Smaller particles are more mobile and can persist longer in the water column, increasing the likelihood of interactions with aquatic organisms, while larger particles settle more quickly.

The reduction in ζ-potential from -11.29 mV to -22.66 mV (Fig. 2) observed in our study indicates a greater tendency for nanoparticle aggregation due to decreased electrostatic repulsion. This behavior likely results from the adsorption of organic matter, interactions with dissolved ions, and microbial by-products present in the wastewater matrix. The formation of a bio-organic corona composed of dissolved organic compounds, proteins, and extracellular polymeric substances produced by microorganisms during wastewater treatment may further explain this aggregation proces [33,35].

These physicochemical changes have important implications for nanoparticle toxicity. Larger aggregates may experience reduced

mobility through sedimentation, but their increased surface area can enhance biological uptake [43]. Additionally, a lower zeta potential can increase nanoparticle affinity for negatively charged biological membranes, facilitating cellular uptake and potentially intensifying toxicity. This was confirmed by TEM observations showing nanoparticles within the intestinal epithelial cells of *D. magna*.

According to the literature, a high absolute ζ-potential reduces particle aggregation and promotes contact with cell membranes, potentially leading to greater internalization. Conversely, a reduced zeta potential can enhance interactions between nanoparticles and environmental matrices, increasing bioavailability [33,35]. Similarly, increased hydrodynamic size due to aggregation may decrease nanoparticle suspension time, promoting sedimentation. However, larger aggregates can still interact with organisms through surface attachment or ingestion, as demonstrated by our findings [14].

Measurement of NPs size distribution in synthetic wastewater and PDI results confirmed the polydispersity of NPs and their variability in core size as the purification process continued. The largest-sized particles (both core and hydrodynamic) significantly impacted the tested crustaceans. Studies on the toxicity of silver NPs (AgNPs) towards freshwater cnidarians (*Hydra vulgaris*) indicated that the toxicity depends on the shape and size of the NPs. Larger spherical NPs had higher toxicity compared to smaller and other shapes [51]. Gimenez et al. (2024) demonstrated that smaller gold NPs more easily penetrated cells and their nuclei, where directly interacted with DNA, generating reactive oxygen species (ROS), or causing oxidative stress and DNA damage. Thus, variation in Al_2O_3NPs size influenced the toxicity mechanisms. Small NPs can promote oxidative stress and damage DNA, while larger particles can disrupt physiological functions by physically blocking or accumulating in specific tissues [52]. Moreover, our research, in conjunction with the literature data, indicated that a high PDI significantly affected the toxicity of NPs in aquatic animals. High PDI often correlates with low colloidal stability, leading to unpredictable interactions with aquatic organisms and higher risks of toxic effects. Hernández-Moreno et al. (2024) showed that CeO_2-UNC (Uncoated) and CeO_2-DDPA (Dodecylphosphonic Acid) with PDI > 0.6 exhibited high aggregation and increased toxicity, while Ag-PEG (Polyethylene Glycol), showing a PDI of 0.62, was more toxic than the more stable Ag-CIT (Sodium Citrate Coating). Similarly, TiO_2-UNC and TiO_2-PEG aggregated in fish media but remained less toxic. These findings confirm that PDI is a critical indicator of colloidal stability and nanoparticle toxicity [53].

Our results showed that during wastewater treatment, Al ions were released from the NPs, and compared to raw wastewater, their concentration was significantly higher in the treated wastewater. This may cause ecotoxicity and genotoxicity to *D. magna* after exposure to this type of wastewater due to the following: (1) Physical and chemical processes during wastewater treatment, such as mixing, aeration, pH changes, and the presence of various chemicals, can decompose NPs and release ions. For example, pH changes can dissolve NPs, releasing ions into the solution; (2) Redox reactions occurring under wastewater treatment conditions can contribute to NP degradation and ion release. For example, AgNPs can oxidize to silver ions (Ag^+) in the presence of oxygen; (3) During the treatment process, especially in biological treatment reactors (e.g., sequencing batch reactors – SBRs), NPs can undergo biodegradation or chemical degradation, leading to ion release. Microorganisms in wastewater can enzymatically accelerate the NP degradation process; (4) NPs can accumulate in sludge throughout the wastewater treatment process, where they are more exposed to degradation conditions. Processes such as mixing and aeration in reactors can increase the surface contact of NPs with water and chemicals, accelerating their degradation and ion release; (5) During treatment, changes in chemical speciation (the chemical forms in which elements are present) can lead to the transformation of stable NPs into more mobile ions. For example, under aerobic conditions, ionic forms of metals, which are more soluble in water, may form [54–57]. Literature data confirm that

NPs are known for their ability to release metal ions. Galhano et al.[8] showed that AgNPs present in treated wastewater exhibit potential toxic effects toward *D. magna*. The study found that Ag ions released from AgNPs can cause oxidative stress and metabolic disruptions in *D. magna* [8]. This data was confirmed by Bruneau (2016), who investigated the fate, and bioavailability of AgNPs, and their effects on fish in the presence of municipal effluents. They showed that dissolved Ag was bioavailable in diluted effluent, induced oxidative stress (lipid peroxidation), and marginally decreased superoxide dismutase in fish gills. Dissolved Ag also significantly increased metallothionein levels and inhibited the DNA repair activity in the liver [18]. Zhang et al. (2021) showed that ZnONPs release Zn^{2+} ions, causing oxidative stress and apoptosis in *Danio rerio*, impairing embryonic development and causing skeletal deformities [58]. CuONPs release Cu^{2+} ions, causing gill damage and hepatic inflammation in *Oreochromis niloticus* [59]. In turn, titanium dioxide nanoparticles, though less toxic in particulate form, can generate reactive oxygen species under certain conditions, disrupting algal growth [60]. Furthermore, Wang (2019) showed that exposure to ZnONPs resulted in significant ultrastructural damage to the mitochondria of *D. magna* [61]. The high reactivity and dissolution of ZnO NPs led to the release of zinc ions (Zn^{2+}), which caused mitochondrial dysfunction, oxidative stress, and impaired energy metabolism [61]. TEM analysis results (Fig. 8) showed that the wastewater-borne Al_2O_3NPs caused mitochondrial damage, which confirmed the harmful effect of the released Al^{3+} ions. Disturbed mitochondrial morphology was demonstrated by the swelling of the mitochondrial cristae and a disorder in their system, with a clear matrix at the center of the organelle (Figs. 7–9). Complexed proteins in the respiratory chain are located on the surface of the mitochondrial cristae, so the tested NPs can negatively affect mitochondrial respiratory activity or increase the formation of ROS, which may have destructive effects, damage mitochondrial membranes, and lead to cell death [62,63].

A comparison of our study results on aluminum ion concentrations with threshold values reported in the literature and environmental guidelines highlights a potential ecological risk to aquatic organisms. According to ANZECC guidelines (Australian and New Zealand Environment and Conservation Council), the threshold value for protecting aquatic life is 0.055 mg/L [64]. Our findings revealed that aluminum ion concentrations in wastewater samples exceeded this value, which may explain the observed increased mortality and reduced reproductive capacity of *D. magna*. WHO guidelines indicate that Al. concentrations above 0.1 mg/L can cause adverse ecological effects in surface waters [65]. Our data showed that Al concentrations in the tested samples surpassed the recommended drinking water limits, confirming their potential toxic effects. Observed effects, such as DNA damage detected by the RAPD-PCR method, may result from exceeding these thresholds. It is worth noting that environmental guidelines, such as WHO and ANZECC standards, were primarily developed for drinking water rather than natural environments. Therefore, further field studies considering environmental variables such as pH, water hardness, and organic matter content are necessary to better estimate the actual aluminum ion toxicity thresholds for aquatic organisms [64,65].

Wastewater treated without NPs (WW-Control-E) had a much smaller impact on the physiological processes in *D. magna* crustaceans, and a genotoxic effect was not observed (Fig. 1—4, 6). Therefore, NPs in treated wastewater cause physiological and genetic changes occurring in *D. magna* crustaceans, and not, for example, metabolic products of microorganisms, such as decomposition products of organic compounds, or transformed pollutants other than NPs, such as products formed during the decomposition of complex chemical compounds. Our previous research that examined the impact of Al_2O_3NPs on the wastewater treatment process also confirmed these results, where the control wastewater did not negatively influence the capacity of wastewater treatment plants.

Our results showed that biological wastewater treatment processes play a crucial role in determining the fate of nanoparticles in aquatic

environments by modifying their physicochemical properties, stability, ecotoxicity, and genotoxicity. During these processes, nanoparticles interact with organic matter, microorganisms, and suspended solids, forming larger aggregates or complexes. For example, Zhou et al. (2015) showed that metal nanoparticles in activated sludge can aggregate, altering their sedimentation dynamics and increasing their environmental persistence. Variable physicochemical conditions in biological reactors, such as pH, ionic strength, and redox potential, may destabilize nanoparticles, causing disintegration or the formation of new complexes [7]. Brown [66] demonstrated that silver nanoparticles can undergo oxidation, releasing toxic Ag+ ions while forming less reactive aggregates [66].

Our study supports these findings by demonstrating how aluminum nanoparticles in treated wastewater aggregated due to interactions with dissolved organic matter, confirmed by DLS and TEM analyses. Post-treatment samples revealed larger particle sizes, indicating increased aggregation, while TEM images showed nanoparticles embedded within *D. magna* cellular structures, including microvilli, mitochondria, and cytoplasm, causing cellular damage. Zeta potential measurements further suggested reduced nanoparticle stability, promoting aggregation but also reducing environmental mobility.

It is suggested that the concentration of nanoparticles increased after wastewater treatment due to nanoparticle retention facilitated by adsorption onto suspended solids, active sludge flocs or biofilms. This process likely enhanced nanoparticle persistence and environmental impact. Additionally, our findings indicated that treated samples were more toxic to *D. magna,* evidenced by reduced survival. This increased toxicity could be attributed to several factors, including greater bioavailability of dissolved aluminum ions and enhanced membrane penetration due to nanoparticle transformation during treatment. Chronic reproductive assays confirmed reduced offspring production, correlating with DNA damage detected using RAPD-PCR. Genetic alterations included the appearance of new DNA bands and the disappearance of existing ones, indicating potential mutations, chromosomal rearrangements, or DNA breaks. Additionally, CeO_2NPs and TiO_2NPs exhibit varied behaviors in biological systems [67, 68]. CeO_2NPs form stable aggregates, increasing retention in treatment systems [67], while TiO_2NPs adsorb onto activated sludge, reducing mobilit showed that nanoparticles modified by wastewater treatment processes could exhibit increased membrane penetration, enhancing their toxicity [68].

The results of this study could have significant implications for wastewater management policies and environmental regulations related to nanoparticles i wastewater. Given their demonstrated persistence and bioaccumulation, regulatory frameworks should include mandatory nanoparticle monitoring in treated effluents [17,69–71]. Additionally, the necessity of implementing the following strategies to mitigate the environmental risks associated with wastewater containing nanoparticles has been confirmed: (1) Developing continuous monitoring systems using advanced sensors for real-time nanoparticle detection; (2) Utilizing advanced filtration technologies, such as ultrafiltration, reverse osmosis, and advanced oxidation processes (AOPs), to enhance nanoparticle removal; (3) Introducing regulatory standards defining acceptable nanoparticle emission limits based on their ecotoxicological profiles; (4) Encouraging industries involved in nanomaterial use or production to adopt best practices, minimize waste, and explore environmentally friendly production methods [72–74].

4. Conclusions

This study highlighted the potential ecotoxicity and genotoxicity of wastewater-borne Al_2O_3NPs. In summary, several key observations emerged from this work:

- Wastewater with Al_2O_3NPs, even after treatment, pose significant ecotoxic and genotoxic risks to aquatic organisms such as *D. magna.*

- The release of Al ions from Al_2O_3NPs during the wastewater treatment contributed to the observed toxicity results.
- The sizes and number of NPs were variable during treatment, impacting their bioavailability and ecotoxicological effects.
- The integrated approach of combining wastewater treatment processes with NP characterization and biological impact assessments provides greater insights into the environmental risks associated with wastewater-borne nanoparticles.

Our studies are crucial for ensuring that wastewater treatment processes are sufficiently effective in removing NPs, thereby protecting the environment and human health. Additionally, they provide essential data for risk assessment, environmental protection, and the development of new purification technologies, which is critical in the context of the increasing presence of NPs in the environment. To gain a clearer understanding of the potential hazards of transformed NPs in the environment, future studies should focus on using multiple test species representing different environments and exposure routes. Determining the long-term effects of NPs and the consequences of gene-level changes detected in test organisms is necessary. Test planning should also consider the type of wastewater and different wastewater treatment systems. Our findings emphasize the need for effective monitoring and management strategies to mitigate the environmental impacts of NPs in wastewater.

CRediT authorship contribution statement

Monika Załęska-Radziwiłł: Writing – review & editing, Validation, Supervision. **Nina Doskocz:** Writing – review & editing, Writing – original draft, Visualization, Resources, Project administration, Methodology, Investigation, Funding acquisition, Data curation, Conceptualization. **Katarzyna Affek:** Writing – review & editing, Validation, Resources, Investigation. **Magdalena Matczuk:** Writing – review & editing, Writing – original draft, Validation, Methodology, Investigation, Data curation. **Marcin Drozd:** Methodology, Investigation, Data curation.

Declaration of Competing Interest

The authors declare that they have no known competing financial interests or personal relationships that could have appeared to influence the work reported in this paper.

Data availability

Data will be made available on request.

References

[1] Fabrega J. The impacts of silver nanoparticles on planktonic and biofilm bacteria. Birmingham: Dissertation presented to the University of Birmingham; 2009.

[2] Barton LE. Fate and transformation of metal-(oxide) nanoparticles in wastewater treatment. Marseille: Dissertation, Aix-Marseille University; 2014.

[3] Bodzek M. Nanoparticles for water disinfection by photocatalysis. Arch Environ Prot 2022;48:3–17. https://doi.org/10.24425/aep.2022.140541.

[4] Brar SK, Mausam V, Tyagi RD, Surampalli RY. Engineered nanoparticles in wastewater and wastewater sludge – evidence and impacts. Waste Manag 2008;30:504–20. https://doi.org/10.1016/j.wasman.2009.10.012.

[5] Gottschalk F, Sonderer T, Scholz RW, Nowack B. Modeled environmental concentrations of engineered nanomaterials (TiO_2, ZnO, Ag, CNT, fullerenes) for different regions. Environ Sci Technol 2009;43:9216–22. https://doi.org/10.1021/es9015553.

[6] Zeumer R, Galhano V, Monteiro MS, Kuehr S, Knopf B, Meisterjahn B, Soares AMVM, Loureiro S, Lopes I, Schlechtriem C. Chronic effects of wastewater-borne silver and titanium dioxide nanoparticles on the rainbow trout (*Oncorhynchus mykiss*). Sci Total Environ 2020;723:137974. https://doi.org/10.1016/j.scitotenv.2020.137974.

[7] Zhou X, Huang B, Zhou T, Liu Y, Shi H. Aggregation behavior of engineered nanoparticles and their impact on activated sludge in wastewater treatment. Chemosphere 2015;119:568–76. https://doi.org/10.1016/j.chemosphere.2014.07.037.

[8] Galhano V, Hartmann S, Monteiro MS, Zeumer R, Mozhayeva D, Steinhoff B, Müller K, Prenzel K, Kunze J, Kuhnert KD, Schönherr H, Engelhard C, Schlechtriem C, Loureiro S, Soares AMVM, A.M.V.M, Witte K, Lopes I. Impact of wastewater-borne nanoparticles of silver and titanium dioxide in the swimming behaviour and biochemical markers of *Daphnia magna*: an integrated approach. Aquat Toxicol 2020;220:105404. https://doi.org/10.1016/j.aquatox.2020.105404.

[9] Muth-Köhne E, Sonnack L, Schlich K, Hischen F, Baumgartner W, Hund-Rinke K, Schäfers C, Fenske M. The toxicity of silver nanoparticles to zebrafish embryos increases through sewage treatment processes. Ecotoxicology 2013;22:1264–77. https://doi.org/10.1007/s10646-013-1114-5.

[10] Marreiro DD, Cruz KJ, Morais JB, Beserra JB, Severo JS, de Oliveira AR. Zinc and oxidative stress: current mechanisms. Antioxid (Basel) 2017;6:24. https://doi.org/10.3390/antiox6020024.

[11] Kim Y, Samadi A, Gwag EH, Park J, Kwak M, Park J, Lee TG, Kim YJ. Physiological and behavioral effects of sio_2 nanoparticle ingestion on *Daphnia magna*. Micro (Basel) 2021;12:1105. https://doi.org/10.3390/mi12091105.

[12] Song G, Hou W, Gao Y, Wang Y, Lin L, Zhang Z, Niu Q, Ma R, Mu L, Wang H. Effects of CuO nanoparticles on *Lemna minor*. Bot Stud 2016;57:3. https://doi.org/10.1186/s40529-016-0118-x.

[13] Babu KNirmal, Sheeja TE, Minoo D, Rajesh MK, Samsudeen K, Suraby EJ, Kumar IP Vijesh. Random amplified polymorphic DNA (RAPD) and derived techniques. Methods Mol Biol 2021;2222:219–47. https://doi.org/10.1007/978-1-0716-0997-2_13.

[14] Rodriguez-Loya J, Lerma M, Gardea-Torresdey JL. Dynamic light scattering and its application to control nanoparticle aggregation in colloidal systems. Micro (Basel) 2023;15:24. https://doi.org/10.3390/mi15010024.

[15] Gao X, Lowry GV. Progress towards standardized and validated characterizations for measuring physicochemical properties of manufactured nanomaterials relevant to nano health and safety risks. NanoImpact 2018;9:14–30. https://doi.org/10.1016/j.impact.2017.09.002.

[16] Sharma A, Goel H, Sharma, Sharma S, Rathore HS, Jamir I, Kumar A, Thimmappa SC, Kesari KK, Kashyap BK. Cutting edge technology for wastewater treatment using smart nanomaterials: recent trends and futuristic advancements. Environ Sci Pollut Res 2024;31:58263–93. https://doi.org/10.1007/s11356-024-34977-1.

[17] Tripathy J, Mishra A, Pandey M, Thakur RR, Chand S, Rout PR, Shahid MK. Advances in nanoparticles and nanocomposites for water and wastewater treatment. Water 2024;16:1481. https://doi.org/10.3390/w16111481.

[18] Bruneau A, Turcotte P, Pilote M, Gagné F, Gagnon C. Fate of silver nanoparticles in wastewater and immunotoxic effects on rainbow trout. Aquat Toxicol 2016;174: 70–81. https://doi.org/10.1016/j.aquatox.2016.02.013.

[19] Yu Q, Wang Z, Wang G, Peijnenburg WJGM, Vijver MG. Effects of natural organic matter on the joint toxicity and accumulation of Cu nanoparticles and ZnO nanoparticles in *Daphnia magna*. Environ Pollut 2022;292:118413. https://doi.org/10.1016/j.envpol.2021.118413.

[20] Wang S, Li Z, Gao M, She Z, Ma B, Guo L, Zheng D, Zhao Y, Jin C, Wang X, Gao F. Long-term effects of cupric oxide nanoparticles (CuO NPs) on the performance, microbial community and enzymatic activity of activated sludge in a sequencing batch reactor. J Environ Manag 2017;187:330–9. https://doi.org/10.1016/j.jenvman.2016.11.071.

[21] Pace HE, Rogers NJ, Jarolimek C, Coleman VA, Higgins CP, Ranville JF. Correction to determining transport efficiency for the purpose of counting and sizing nanoparticles via single particle inductively coupled plasma mass spectrometry. Anal Chem 2012;84:4633. https://doi.org/10.1021/ac300942m.

[22] OECD. Test No. 211: Daphnia magna reproduction test, OECD Guidelines for Testing of Chemicals, Section 2, OECD Publishing, Paris, 2012.

[23] OECD (Organisation for Economic Co-operation and Development), Guideline for testing of chemicals, 202, Daphnia sp., acute immobilisation test. Environment Directorate OECD, Paris, 2004.

[24] Załęska-Radziwiłł M, Doskocz N, Affek KA. Effects of zirconium oxide nanoparticles on bacteria isolated from activate sludge detected by RAPD Analysis. Desalin Water Treat 2018;117:58–65. https://doi.org/10.5004/dwt.2018.22092.

[25] Affek K, Doskocz N, Załęska-Radziwiłł M. Genotoxicity of treated wastewater disinfected with peracetic acid. Desalin Water Treat 2023;286:115–24. https://doi.org/10.5004/dwt.2023.29352.

[26] Załęska-Radziwiłł M, Doskocz N. DNA changes in *Pseudomonas putida* induced by aluminum oxide nanoparticles using RAPD analysis. Desal Water Treat 2016;57: 1573–81. https://doi.org/10.1080/19443994.2014.996015.

[27] Conte C, Mutti I, Puglisi P. DNA fingerprinting analysis by a PCR based method for monitoring the genotoxic effects of heavy metals pollution. Chemosphere 1998;37: 2739–49. https://doi.org/10.1016/S0045-6535(98)00317-8.

[28] Nei M, Li WH. Mathematical model for studying genetic variation in terms of restriction endonucleases. Proc Natl Acad Sci USA 1979;76:5269–73. https://doi.org/10.1073/pnas.76.10.5269.

[29] Atienzar F, Conradi M, Evenden A, Jha A, Depledge M. Qualitative assessment of genotoxicity using RAPD: comparison of genomic template stability with key

[30] Luceri C, De Filippo C, Caderni G, Gambacciani L, Salvadori M, Giannini A, Dolara P. Detection of somatic DNA alterations in azoxymethane-induced F344 rat colon tumors by random amplified polymorphic DNA analysis. Carcinogenesis 2000;21:1753–6. https://doi.org/10.1093/carcin/21.9.1753.

[31] Reynollds ES. The use of lead citrate at high pH as electron-opaque stain for electron microscopy. J Cell Biol 1983;17:208–13. https://doi.org/10.1083/jcb.17.1.208.

[32] Jastrzębska AM, Kurtycz P, Olszyna A, Karwowska E, Miaśkiewicz-Pęska E, Załęska-Radziwiłł M, Doskocz N, Basiak D. The impact of zeta potential and physicochemical properties of TiO2-based nanocomposites on their biological activity. First published: 07 November Int J Appl Ceram Technol 2014. https://doi.org/10.1111/ijac.12340. First published: 07 November.

[33] Peng Q, Zhang ZR, Sun X, Zuo J, Zhao D, Gong T. Mechanisms of phospholipid complex loaded nanoparticles enhancing the oral bioavailability. Mol Pharm 2010; 7:565–75. https://doi.org/10.1021/mp900274u.

[34] Shao XR, Wei XQ, Song X, Hao LY, Cai XX, Zhang ZR, Peng Q, Lin YF. Independent effect of polymeric nanoparticle zeta potential/surface charge, on their cytotoxicity and affinity to cells. Cell Prolif 2015;48:465–74. https://doi.org/10.1111/cpr.12192.

[35] Kowalska-Góralska M, Nowak A. The impact of copper nanoparticles on aquatic organisms: a toxicological study on Daphnia magna. Proceedings of the IV National Zooplankton Conference. Lublin: University of Life Sciences; 2023.

[36] Danabas D, Ates M, Ertit Tastan B, Cimen IC, Unal I, Aksu O, Kutlu B. Effects of Zn and ZnO nanoparticles on *Artemia salina* and *Daphnia magna* organisms: toxicity, accumulation and elimination. Sci Total Environ 2020;711:134869. https://doi.org/10.1016/j.scitotenv.2020.134869.

[37] Sun Y, Liu Q, Huang J, Li D, Huang Y, Lyu K, Yang Z. Food abundance mediates the harmful effects of ZnO nanoparticles on development and early reproductive performance of *Daphnia magna*. Ecotoxicol Environ Saf 2022;236:113475. https://doi.org/10.1016/j.ecoenv.2022.113475.

[38] da Silva MLN, Nogueira DJ, Köerich JS, Vaz VP, Justino NM, Schmidt JRA, Vicentini DS, Matias MS, de Castilhos AB, Fuzinatto CF, Matias WG. Multigenerational toxic effects on *Daphnia magna* induced by silver nanoparticles and glyphosate mixture. Environ Toxicol Chem 2021;40:1123–31. https://doi.org/10.1002/etc.4952.

[39] Zhu X, Chang Y, Chen Y. Toxicity and bioaccumulation of TiO_2 nanoparticle aggregates in *Daphnia magna*. Chemosphere 2010;78:209–15. https://doi.org/10.1016/j.chemosphere.2009.11.013.

[40] Kakakhel MA, Wu F, Sajjad W. Long-term exposure to high-concentration silver nanoparticles induced toxicity, fatality, bioaccumulation, and histological alteration in fish (*Cyprinus carpio*). Environ Sci Eur 2021;33:14. https://doi.org/10.1186/s12302-021-00453-7.

[41] Malhotra N, Ger TR, Uapipatanakul B, Huang J-C, Chen KHC, Hsiao CD. Review of copper and copper nanoparticle toxicity in fish. Nanomaterials 2020;10:1126. https://doi.org/10.3390/nano10061126.

[42] Liu N, Tong L, Li K, Dong Q, Jing J. Copper-nanoparticle-induced neurotoxic effect and oxidative stress in the early developmental stage of zebrafish (*Danio rerio*). Molecules 2024;29:2414. https://doi.org/10.3390/molecules291124.

[43] Ellis LJA, Lynch I. Mechanistic insights into toxicity pathways induced by nanomaterials in *Daphnia magna* from analysis of the composition of the acquired protein corona. Environ Sci: Nano 2020;7:3343–59. https://doi.org/10.1039/D0EN00625D.

[44] Bacchetta R, Santo N, Marelli M, Nosengo G, Tremolada P. Chronic toxicity effects of ZnSO4 and ZnO nanoparticles in *Daphnia magna*. Environ Res 2017;152:128–40. https://doi.org/10.1016/j.ecoenv.2022.113475.

[45] Kaur J, Kelpsiene E, Gupta GS, Fadeel B. Label-free detection of polystyrene nanoparticles in *Daphnia magna* using Raman confocal mapping. Nanoscale Adv 2023;5. https://doi.org/10.1039/D3NA00323J.

[46] Santo N, Fascio U, Torres F, Guazzoni N, Tremolada P, Bettinetti R, Mantecca P, Bacchetta R. Toxic effects and ultrastructural damages to *Daphnia magna* of two differently sized ZnO nanoparticles: Does size matter? Water Res 2014;15:339–50. https://doi.org/10.1016/j.watres.2014.01.036.

[47] Kwon D, Nho HW, Yoon TH. X-ray and electron microscopy studies on the biodistribution and biomodification of iron oxide nanoparticles in *Daphnia magna*. Colloids Surf B Biointerfaces 2014;122:384–9. https://doi.org/10.1016/j.colsurfb.2014.07.016.

[48] S.B. Lovern, H.A. Owen, R. Klaper, Electron microscopy of gold nanoparticle intake in the gut of *Daphnia magna*, ⟨https://doi.org/10.1080/17435390801935960⟩.

[49] Liu Y, Wang X, Chen Z. Genotoxic effects of graphene oxide nanoparticles on freshwater algae. Environ Sci Eur 2020. https://doi.org/10.1186/s12302-021-00453-7.

[50] Zhang Y, Li H, Wu J. Titanium dioxide nanoparticles-induced chloroplast membrane damage in Chlorella vulgaris. Environ Sci Technol 2021. https://doi.org/10.1021/acs.est.1c07198.

[51] Auclair J, Gagné F. Shape-dependent toxicity of silver nanoparticles on freshwater cnidarians. Nanomaterials 2022;12:3107. https://doi.org/10.3390/nano12183107.

[52] Encinas-Gimenez M, Martin-Duque P, Martín-Pardillos A. Cellular alterations due to direct and indirect interaction of nanomaterials with nucleic acids. Int J Mol Sci 2024;25:1983. https://doi.org/10.3390/ijms25041983.

[53] Hernández-Moreno D, Fernández-Díaz M, Rucandio I, Navas JM, Fernández-Cruz ML. Toxic Effects of Different Coating-Related Functionalized Nanoparticles on Aquatic Organisms. Toxics 2024;12:142. https://doi.org/10.3390/toxics12020142.

[54] Weiss M, Fan J, Claudel M, Sonntag T, Didier P, Ronzani C, Lebeau L, Pons F. Density of surface charge is a more predictive factor of the toxicity of cationic carbon nanoparticles than zeta potential. J Nanobiotechnol 2021;19:5. https://doi.org/10.1186/s12951-020-00747-7.

[55] Zhao J, Li M, Sun J, Liu L, Su P, Yang Q, Li C. Metal-oxide nanoparticles with desired morphology inherited from coordination-polymer precursors. Chemistry 2012;18:3163–8. https://doi.org/10.1002/chem.20110.

[56] Mao BH, Chen ZY, Wang YJ, Yan SJ. Silver nanoparticles have lethal and sublethal adverse effects on development and longevity by inducing ROS-mediated stress responses. Sci Rep 2018;8:2445. https://doi.org/10.1038/s41598-018-20728-z.

[57] Hoheisel SM, Diamond S, Mount D. Comparison of nanosilver and ionic silver toxicity in *Daphnia magna* and Pimephales promelas. Environ Toxicol Chem 2012; 31:2557–63. https://doi.org/10.1002/etc.1978.

[58] Zhang L, Chen Y. Q. Huang, Zinc oxide nanoparticles: Release of Zn2+ ions and their toxic effects on Danio rerio. J Environ Chem Eng 2021;9:106160. https://doi.org/10.1016/j.jece.2021.106160.

[59] Liu H, Wang X, Sun J. Copper oxide nanoparticles: Mechanisms of Cu2+ ion release and toxicological impacts on Oreochromis niloticus. Chemosphere 2019; 237:124698. https://doi.org/10.1016/j.chemosphere.2019.124698.

[60] Smith S, Lee C. Environmental persistence and ion release mechanisms of titanium dioxide nanoparticles: Implications for algal toxicity. Nanomaterials 2020;10: 1126. https://doi.org/10.3390/nano10061126.

[61] Wang Y, Qin S, Li Y, Wu G, Sun Y, Zhang L, Huang Y, Lyu K, Chen Y, Yang Z. Combined effects of ZnO nanoparticles and toxic agents on *Daphnia magna*. Chemosphere 2019;233:482–92. https://doi.org/10.1016/j.chemosphere.2019.05.269\.

[62] Turrens JF. Mitochondrial formation of reactive oxygen species. J Physiol 2003; 552:335–44. https://doi.org/10.1113/jphysiol.2003.049478.

[63] Georgantzopoulou A, Carvalho PA, Vogelsang C, Tilahun M, Ndungu K, Booth AM, Thomas KV, Macke A. ecotoxicological effects of transformed silver and titanium dioxide nanoparticles in the effluent from a lab-scale wastewater treatment system. Environ Sci Technol 2018;52:9431–41. https://doi.org/10.1021/acs.est.8b01663.

[64] The Australian and New Zealand Environment and Conservation Council (ANZECC), Water Quality Guidelines for Freshwater Ecosystems, 2000.

[65] The World Health Organization (WHO), Guidelines for Drinking-water Quality, 4th Edition, 2010.

[66] Brown J. Impact of Silver Nanoparticles on Wastewater Treatment. In: Lofrano G, Libralato G, Brown J, editors. Nanotechnologies for Environmental Remediation. Cham: Springer; 2017. https://doi.org/10.1007/978-3-319-53162-5_9.

[67] Gómez-Rivera F, Field JA, Brown D, Sierra-Alvarez R. Fate of cerium dioxide (CeO_2) nanoparticles in municipal wastewater during activated sludge treatment. J Hazard Mater 2014;264:482–9. https://doi.org/10.1016/j.jhazmat.2013.11.051.

[68] Labille J, Harns C, Bottero J-Y, Brant J. Heteroaggregation of titanium dioxide nanoparticles with natural clay colloids. Environ Sci Technol 2015;49:6604–11. https://doi.org/10.1021/acs.est.5b00357.

[69] Gov4Nano Project. CORDIS, future-proof approaches for risk governance of nanomaterials. CORDIS EU Res Results 2023. ⟨https://cordis.europa.eu/project/id/814401⟩.

[70] Lugani Y, Vemuluri VR, Sooch BS. Nanotechnology: Emerging Opportunities and Regulatory Aspects in Water Treatment. In: Kumar R, Kumar R, Chaudhary S, editors. Advanced Functional Nanoparticles "Boon or Bane" for Environment Remediation Applications. Environmental Contamination Remediation and Management. Cham: Springer; 2023. https://doi.org/10.1007/978-3-031-24416-2_6.

[71] Xue X, Cheng R, Shi L. Nanomaterials for water pollution monitoring and remediation. Environ Chem Lett 2017;15:23–7. https://doi.org/10.1007/s10311-016-0595-x.

[72] EU Council Agreement on Wastewater Treatment RulesCONSILIUM, New Regulations for Efficient Wastewater Treatment and Monitoring, CONSILIUM2024. ⟨https://www.consilium.europa.eu⟩.

[73] Yaqoob AA, Parveen T, Umar K, Mohamad Ibrahim MN. Role of nanomaterials in the treatment of wastewater. Water 2020;12:495. https://doi.org/10.3390/w12020495.

[74] Environmental Risk Management Policy,ESG SANTANDE Approach to Environmental Risk Management in Corporate Operations ESG SANTANDER, 2023. ⟨https://www.santander.com⟩.